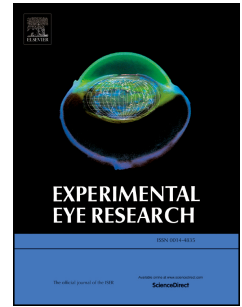


# Journal Pre-proof

Depth-dependent mechanical properties of the human cornea by uniaxial extension

Malavika H. Nambiar, Theo G. Seiler, Sebastian Senti, Layko Liechti, Fabian Müller, Harald Studer, Abhijit S. Roy, Philippe Büchler



PII: S0014-4835(23)00339-1

DOI: <https://doi.org/10.1016/j.exer.2023.109718>

Reference: YEXER 109718

To appear in: *Experimental Eye Research*

Received Date: 14 July 2023

Revised Date: 13 October 2023

Accepted Date: 6 November 2023

Please cite this article as: Nambiar, M.H., Seiler, T.G., Senti, S., Liechti, L., Müller, F., Studer, H., Roy, A.S., Büchler, P., Depth-dependent mechanical properties of the human cornea by uniaxial extension, *Experimental Eye Research* (2023), doi: <https://doi.org/10.1016/j.exer.2023.109718>.

This is a PDF file of an article that has undergone enhancements after acceptance, such as the addition of a cover page and metadata, and formatting for readability, but it is not yet the definitive version of record. This version will undergo additional copyediting, typesetting and review before it is published in its final form, but we are providing this version to give early visibility of the article. Please note that, during the production process, errors may be discovered which could affect the content, and all legal disclaimers that apply to the journal pertain.

© 2023 Published by Elsevier Ltd.

# 1 Depth-dependent mechanical properties 2 of the human cornea by uniaxial extension

3 **Malavika H. Nambiar<sup>1</sup>, Theo G. Seiler<sup>2,3,4</sup>, Sebastian Senti<sup>1</sup>, Layko Liechti<sup>5</sup>, Fabian Müller<sup>5</sup>**  
4 **Harald Studer, Abhijit S. Roy<sup>6</sup>, Philippe Büchler<sup>1</sup>**

5 1. ARTORG Center for Biomedical Engineering Research, University of Bern, Freiburgstrasse 3,  
6 3010 Bern, Switzerland

7 2. IROC AG, Institut für Refraktive und Ophthalgo-Chirurgie, Stockerstrasse 37, 8002 Zürich,  
8 Switzerland

9 3. Universitätsklinik für Augenheilkunde, Inselspital Bern, Freiburgstrasse 15, 3010 Bern,  
10 Switzerland

11 4. Klinik für Augenheilkunde, Universitätsklinikum Düsseldorf, Moorenstr. 5, 40225 Düsseldorf,  
12 Deutschland

13 5. Ziemer Ophthalmic Systems AG, Allmendstrasse 11, 2562 Port, Switzerland

14 6. Narayana Nethralaya Eye Clinic, Bengaluru, Karnataka 560010, India

15  
16 Malavika H. Nambiar – malavika.nambiar@unibe.ch

17 Theo G. Seiler – theo@seiler.tv

18 Sebastian Senti – Sebastian.senti@unibe.ch

19 Layko Liechti – Layko.Liechti@ziemergroup.com

20 Fabian Müller – fabian.mueller@ziemergroup.com

21 Harald Studer – harald.studer@gmail.com

22 Abhijit S. Roy – asroy27@yahoo.com

23 Philippe Büchler – philippe.buechler@unibe.ch

24

25 **ABSTRACT**

26 The purpose of this study was to investigate the depth-dependent biomechanical properties of the  
27 human corneal stroma under uniaxial tensile loading. Human stroma samples were obtained after the  
28 removal of Descemet's membrane in the course of Descemet's membrane endothelial keratoplasty  
29 (DMEK) transplantation. Uniaxial tensile tests were performed at three different depths: anterior,  
30 central, and posterior on 2 x 6 x 0.15 mm strips taken from the central DMEK graft. The measured  
31 force-displacement data were used to calculate stress-strain curves and to derive the tangent  
32 modulus. The study showed that mechanical strength decreased significantly with depth. The anterior  
33 cornea appeared to be the stiffest, with a stiffness approximately 18% higher than that of the central  
34 cornea and approximately 38% higher than that of the posterior layer. Larger variations in mechanical  
35 response were observed in the posterior group, probably due to the higher degree of alignment of the  
36 collagen fibers in the posterior sections of the cornea. This study contributes to a better understanding  
37 of the biomechanical tensile properties of the cornea, which has important implications for the  
38 development of new treatment strategies for corneal diseases. Accurate quantification of tensile  
39 strength as a function of depth is critical information that is lacking in human corneal biomechanics to  
40 develop numerical models and new treatment methods.

41

42 **Keywords:** Human cornea, tensile testing, depth-dependent, uniaxial testing.

## 43 1. INTRODUCTION

44 Over 185,000 corneal transplant surgeries are performed annually worldwide, yet, 53% of the world's  
45 population does not have access to donor corneas, which also limits their availability for research  
46 (Bunya et al., 2023). Understanding the biomechanical properties of the cornea can help us develop  
47 more effective surgical interventions and treatment strategies that can restore corneal integrity and  
48 prevent the progression of corneal diseases. It is critical to understand the biomechanics of this  
49 complex tissue, which is highly anisotropic, heterogeneous, and multi-layered. Knowledge of the  
50 tensile strength of the cornea can help improve treatment strategies for conditions that affect the  
51 structural integrity of the cornea, such as keratoconus, corneal ectasia, and corneal ulcers. For  
52 example, measuring corneal resistance to deformation or stress can help us determine the optimal  
53 parameters for corneal crosslinking to strengthen corneal tissue in keratoconus, or design  
54 keratotomies to appropriately reduce corneal astigmatism. In addition, studying the tensile strength  
55 of corneal tissue can also contribute to the development of new biomaterials, implants and surgical  
56 techniques for corneal reconstruction and transplantation (Roberts, 2016).

57 While full-thickness tensile testing has been performed on human corneal strips (Elsheikh et al., 2008;  
58 Hoeltzel et al., 1992; Mahdian et al., 2021), there is limited information in the literature on the depth-  
59 dependent biomechanics of the human cornea, particularly on tensile properties. Existing studies on  
60 depth dependence have been performed using shear (Petsche et al., 2012; Sloan et al., 2014),  
61 compression (Ramirez-Garcia et al., 2018), cohesive tension (Randleman et al., 2008), and indentation  
62 (Labate et al., 2015) methods. Physiologically, however, the cornea is subjected to tension due to the  
63 intraocular pressure, which is most important for understanding its biomechanics.

64 Therefore, this study aims to characterize the mechanical properties of the human corneal stroma at  
65 different depths, corresponding to the anterior, central, and posterior corneal stroma by uniaxial  
66 extension. To our knowledge, this is the first depth-dependent uniaxial tensile study performed on

67 human corneas. To control sample preparation, strips were cut with a femtosecond laser to ensure  
68 uniform geometry and thickness and to precisely control the depth of sample extraction.

69

Journal Pre-proof

## 70 MATERIALS AND METHODS

### 71 2.1 Experimental setup

72 Nine human donor corneas (age 55-79 years) were examined in this study. Since good quality corneal  
73 tissue is scarce, this study used corneas after the removal of Descemet's membrane (DM) for DMEK  
74 surgery. The corneas including a 3 mm scleral ring, were provided by the Department of  
75 Ophthalmology of the Inselspital Bern immediately after peeling the DM, which was performed  
76 without damaging the posterior corneal stroma. Before DM peeling, the corneas were examined for  
77 corneal scars and de-swollen in Carry-C (Alchimia, Italy) for 24 hours. After DM peeling, the corneas  
78 were placed in a hydration preserving culture medium containing 5 % Dextran solution. Since this  
79 study used tissue from deceased donors that would otherwise be discarded, the IRB (Cantonal Ethics  
80 Committee of the Canton of Bern) granted exempt status. The orientation of the corneas were  
81 unknown.

82 Within 72 hours after DM peeling, the cornea was placed in an artificial anterior chamber  
83 pressurization device with the corneal epithelium side facing upward to prevent movement during  
84 strip cutting with the Femto LDV Z8 Neo femtosecond laser (Ziemer Ophthalmic Systems AG,  
85 Switzerland) (Figure 1). The laser handpiece was centered on the cornea using the OCT integrated into  
86 the device and moved only after all strips were cut. The OCT was also used to measure the total corneal  
87 thickness. The average central corneal thickness in this study was 770  $\mu\text{m}$ . The high thickness variation  
88 can be attributed to swelling, despite the deswelling media due to lack of the endothelium layer. For  
89 each eye, three strips 6 mm long, 2 mm wide, and 0.15 mm thick were cut in the central-corneal region  
90 from the anterior (D1), central (D2), and posterior (D3) thirds of the cornea. No epithelium was present  
91 on the prepared samples. In all but two samples, the first 100  $\mu\text{m}$  of cornea were discarded to ensure  
92 that the Bowmann's membrane was not included in the test. In the two excluded samples, it was not  
93 possible to omit this layer because of low corneal thickness, so the anterior sample (D1) was taken  
94 just below the epithelium. However, no differences were observed in the tests. The samples were

95 individually preserved and tested in a hydration-preserving culture medium containing 5 % Dextran to  
 96 maintain the sample dimensions after cutting (Hamon et al., 2021; Wolf et al., 2009).

97 The strips were uniaxially tested in a bath containing the same culture medium using the Ustretch  
 98 device (CellScale, Waterloo, Canada) at room temperature (Figure 2). The tissue was pre-stretched  
 99 with a low force of 10 mN to ensure uniform tension across the samples. The samples were then  
 100 loaded with 6 cycles at a strain rate of 0.16 % /s. The fifth cycle of force-displacement data was  
 101 recorded for analysis as the mechanical response of the tissue stabilized after the fifth preconditioning  
 102 cycle. The specimens were tested up to a strain of 10 %, which is consistent with previous experiments  
 103 (Boschetti et al., 2012; Elsheikh et al., 2011, 2008; Wollensak et al., 2003). The actual length of the  
 104 specimen was used to calculate the strain, taking into account the distance between the grips under  
 105 the pre-stretch 10 mN, which differs from the original distance of 5 mm due to the initial tensioning  
 106 of the testing device and the unfolding of the specimen. For this reason, the reference length of the  
 107 sample was calculated as the actual distance of the grip at the start of the 5th cycle. The strain was  
 108 then calculated as the ratio of extension to this reference length of the sample. The stress was  
 109 determined by dividing the force by the original cross-sectional area, specifically the product of the  
 110 thickness of the sample (0.15 mm) and the width at the attachment of the rakes (1.56 mm).

111 The relationship between stress and strain was further characterized using an exponential function  
 112 based on a previously proposed method for studying corneal inflation (Eliasy et al., 2019; Elsheikh et  
 113 al., 2010):

$$114 \quad \sigma = A(e^{B(\varepsilon - \varepsilon_0)} - 1) \quad (1)$$

115 Here, A and B are material parameters, and  $\varepsilon_0$  is determined such that the stress corresponds to our  
 116 experimental measurement at zero strain. This additional strain is necessary to account for the initial  
 117 experimental pre-stress introduced to remove the initial compliance of the measurement setup.  
 118 Finally, the stiffness of the specimen was calculated as the derivative of the fitted exponential function  
 119 and used to quantify the stiffness ratio between the different depths.

**120 2.2 Statistical Methods**

121 Statistical analysis was performed using Python 3.7 (Scipy.stats). The uniaxial force and extension data  
122 were used to generate stress-strain curves for each depth and sample. Tangent moduli were  
123 calculated for the low (2 %), intermediate (5 %), and high-strain (10 %) regions of the curves,  
124 corresponding to the stiffness of the tissue at different depths. A one-way ANOVA was performed on  
125 the tangent moduli data for each depth group to analyze the difference between depths. Due to  
126 sample exclusion during experimental measurements, our sample size was insufficient to perform  
127 paired statistical tests. A Tukey post hoc test was used to determine which groups were significantly  
128 different. A p-value of  $< 0.05$  was considered significant.



129 **2. RESULTS**

130 Twenty-seven strips were cut from the 9 donor corneas, but 4 strips were excluded from analysis,  
131 bringing the total number of samples for all groups to 23. The main reason for exclusion was damage  
132 to the sample – usually in the area of attachment – or loosening at the attachment points. 7 samples  
133 were available in the D1 group, and 8 in each of the D2 and D3 groups.

134 The force-displacement behavior during uniaxial measurement was determined for the three depths.  
135 The corresponding stress-strain data was calculated from the measurements (Figure 3). Besides the  
136 typical viscous and nonlinear relationship, our results showed that the mechanical properties of the  
137 stroma decreased with depth, with the anterior D1 group having the highest force, then the central  
138 D2 layer, and the lowest in the posterior D3 stromal layer. The highest variability in stress was  
139 observed in the D3 group (Figure 3). Statistically, D1 and D2 showed a significant difference in force  
140 ( $p < 0.001$ ), as did D2 and D3 ( $p < 0.001$ ) and D1 and D3 ( $p < 0.001$ ). An average maximum force of  
141 0.22 N was observed in the D1 group, 0.18 N in the D2 group and 0.14 N in the D3 group at 10 % strain.  
142 This corresponds to a decrease of 18 % mechanical strength in the central layer (D2) and a 36 % in the  
143 posterior layer (D3), as compared to the anterior layer (D1).

144 The stress- strain data were used to calculate the tangent modulus at 2 %, 5 % and 10 % strain. The  
145 average stress at 10 % strain was used to calculate the difference in mechanical strength between the  
146 three layers. A linear decrease in mechanical properties was observed across depth. The tangent  
147 moduli were evaluated at different strain levels (Figure 4). At 5 % strain, groups D2 and D3 showed no  
148 significant difference ( $p = 0.051$ ), but at 10 % this changed to a significant difference ( $p < 0.001$ ). At all  
149 strains, the tangent modulus was significantly higher at D1 than D2 and D3 ( $p < 0.001$ ). We found no  
150 correlation of tangent modulus with age or thickness.

151 Exponential fitting of stress-strain data showed good agreement with experimental data for all the  
152 depths (Figure 3). Interestingly, the value of exponent B remains nearly constant across different  
153 depths, implying that the mechanical properties between depths are primarily determined by the

154 linear parameter A over a strain range from 0% to 10% (Table 1). The relative change in corneal  
155 stiffness between depths was quantified by calculating the normalized stiffness with respect to the  
156 anterior depth. Since the exponential parameter B remains constant at all depths, this relationship is  
157 nearly constant at each strain level. Furthermore, stiffness decreases linearly from the anterior to the  
158 posterior. The central cornea has a stiffness of about 80% of the anterior stiffness, while the posterior  
159 layer is 60% (Figure 5).

160

Journal Pre-proof

**161 3. DISCUSSION**

162 The objective of this study is to characterize the mechanical properties of the human corneal stroma  
163 at different depths, corresponding to the anterior, central, and posterior cornea by uniaxial extension.  
164 The study aims to understand the depth-dependent biomechanical behavior of the cornea under  
165 tensile loading, which is one of the most relevant loading situation for physiological conditions (Kling  
166 et al., 2020). While the physiological intraocular pressure is better represented by a biaxial setting,  
167 uniaxial testing is a widely used method for estimating tensile mechanics. This study is the first to  
168 characterize the depth-dependent biomechanics of the human cornea under tensile loading. It should  
169 contribute to a better understanding of the biomechanical properties of the cornea and allow the  
170 development of new treatment strategies for corneal diseases.

171 In this study, a linear decrease in tensile mechanical strength was observed across the depth of the  
172 cornea. The central layer was found to be 18 % weaker than the anterior cornea and the posterior  
173 cornea was found to be 38 % weaker than the anterior cornea.

174 Other depth-dependent mechanical characterizations found in the literature include shear (Petsche  
175 et al., 2012; Sloan et al., 2014), compression (Ramirez-Garcia et al., 2018), cohesive tensile (Randleman  
176 et al., 2008), and indentation (Labate et al., 2015). Direct comparison of measured properties is not  
177 possible because the metric used to characterize the mechanical response is different for each test  
178 method. Qualitatively, all these studies found significant stiffer properties for anterior cornea than the  
179 posterior cornea. However, these studies report that the central stroma is mechanically similar to the  
180 posterior cornea, which is different from our results, where significant differences in the mechanical  
181 behavior were observed at all measurement depth – anterior, central, and posterior – with the  
182 stiffness linearly decreasing across depth. This difference in analysis may be attributed to the type of  
183 loading applied to samples in the different tests. The tensile strength of the collagen bundles is the  
184 primary contributor to the uniaxial forces, which is orders of magnitude higher in tension than in  
185 compression. As such, compression tests predominantly characterize the response of the stromal

186 matrix rather than the properties of the collagen fiber, which can explain these differences (Sun,  
187 2021).

188 In this study, the posterior cornea was found to be 38% less stiff than the anterior cornea, which is in  
189 a similar range to the depth dependent tensile mechanics of the porcine cornea (Nambiar et al., 2022).  
190 The central layer was found to be 18% less stiff than the anterior cornea, which was different from  
191 the trends in the porcine cornea that showed a similar mechanical strength of the central and anterior  
192 layers (Nambiar et al., 2022). Comparing the results of this study with uniaxial measurements on full  
193 thickness human corneal strips show that stresses of full thickness measurements are in the range of  
194 D2-D3 groups of this study (Elsheikh, A. et al., 2008; Hoeltzel et al., 1992; Mahdian et al., 2021). The  
195 deviations can be attributed to the depth dependence of the material and to differences in the test  
196 setup, such as clamping and preconditioning. The parameters obtained by fitting the exponential  
197 function indicate a more linear response of the tissue compared with the values published for inflation  
198 experiments (Eliasy et al., 2019; Elsheikh et al., 2010). This difference could be due to the different  
199 loading methods used in the two studies, especially since the inflation experiments reflect a  
200 predominantly biaxial loading scenario. This comparison indicates that uniaxial tests should be  
201 combined with biaxial loading to obtain a comprehensive description of the corneal mechanical  
202 response.

203 Accurate quantification of the tensile strength in a depth-controlled manner is critical information that  
204 is lacking in current numerical models developed to study various refractive interventions (Ariza-  
205 Gracia et al., 2017; Pandolfi and Manganiello, 2006; Sinha Roy et al., 2014; Studer et al., 2010). Even  
206 if the mechanical properties identified in this study corresponds to aged corneas, the trends of  
207 reduction in strength quantified in this study can be reproduced for applications in the young cornea,  
208 which is supported by imaging data and the other mechanical tests in literature (Labate et al., 2015;  
209 Petsche et al., 2012; Ramirez-Garcia et al., 2018; Randleman et al., 2008; Sloan et al., 2014).

210 Looking at the ultrastructure of the human cornea, we see that collagen fibers of the anterior stroma  
211 are randomly dispersed in the plane of the cornea and aligned along the curvature (Quantock et al.,  
212 2007). This in-plane dispersion becomes preferentially oriented in the nasal-temporal and superior-  
213 inferior directions with increasing depth, while preserving some level of isotropic scatter (Abass et al.,  
214 2015; Quantock et al., 2007). However, the posterior cornea exhibits lower mechanical properties,  
215 which seems contradictory because the fibers carry most of the load. This behavior could indicate  
216 lower fiber density in the posterior cornea. The lower stiffness could also be due to a greater out-of-  
217 plane dispersion of the fibers in the posterior cornea, resulting in a lower contribution of the fibers to  
218 the tensile stress. It is plausible that a combination of these elements are at play.

219 This also makes the lack of orientation markers on the donor tissue a limitation of this study for the  
220 posterior group (D3), and a possible explanation for the larger variability in the properties measured  
221 in this group. Another reason for the larger variability observed in the mechanical measurements in  
222 the posterior group could be related to fact the posterior stroma is more susceptible to swelling (Meek  
223 et al., 2003; Wang et al., 2004), especially after removal of the DM. Although care was taken to  
224 maintain the level of hydration of the specimens during testing, the corneas remained slightly swollen  
225 when the specimens were cut from the cornea with the laser. This problem is common in ex vivo  
226 mechanical testing. Although this may result in a slight underestimation of the measured stresses, the  
227 trends and magnitude of the decrease in mechanical strength with depth remain valid. Another  
228 simplification in this study is the assumption that the strips are flat, although the cornea has a  
229 curvature. However, we suspect that the effect on the measured properties is small because of the  
230 small dimensions of the specimens-particularly their thickness-and the fact that they flatten under  
231 their own weight when attached to the experimental setup. Since the corneas were obtained from  
232 transplant tissue, they were from elderly donors, which limits the measured properties to the elderly  
233 population and prevents conclusions about age-dependent mechanical behavior. We found no  
234 correlation of tangent modulus with age, which may be attributed to the limited age variation within  
235 the measured samples.

236 This study contributes to the growing body of knowledge on the biomechanics of the human cornea  
237 by quantifying the depth-dependent tensile biomechanics. This work also highlights the importance  
238 of considering depth-dependent mechanical properties when planning and evaluating corneal  
239 treatments. The results from this study could inform the development of better numerical models for  
240 refractive interventions and improve our understanding of corneal diseases. The method by which  
241 corneal stroma was derived in this study from DMEK surgical waste can be an important source of  
242 corneal stroma for future research.

#### 243 **FUNDING**

244 This study was funded by the SNSF grant (No. IZLIZ3\_182975). There are no conflicts of interests.

245

246 **REFERENCES**

- 247 Abass, A., Hayes, S., White, N., Sorensen, T., Meek, K.M., 2015. Transverse depth-dependent changes  
248 in corneal collagen lamellar orientation and distribution. *J. R. Soc. Interface* 12.  
249 <https://doi.org/10.1098/rsif.2014.0717>
- 250 Ariza-Gracia, M., Ortillés, Cristóbal, J., Rodríguez Matas, J.F., Calvo, B., 2017. A numerical-experimental  
251 protocol to characterize corneal tissue with an application to predict astigmatic keratotomy  
252 surgery. *J. Mech. Behav. Biomed. Mater.* 74, 304–314.  
253 <https://doi.org/10.1016/j.jmbbm.2017.06.017>
- 254 Boschetti, F., Triacca, V., Spinelli, L., Pandolfi, A., 2012. Mechanical characterization of porcine  
255 corneas. *J. Biomech. Eng.* 134, 1–9. <https://doi.org/10.1115/1.4006089>
- 256 Bunya, V.Y., Syed, Z.A., Puente, M.A., 2023. EyeWiki- American Academy of Ophtalmology [WWW  
257 Document]. URL [https://eyewiki.aao.org/Corneal\\_Donation](https://eyewiki.aao.org/Corneal_Donation)
- 258 Eliasy, A., Chen, K.-J., Vinciguerra, R., Lopes, B.T., Abass, A., Vinciguerra, P., Ambrósio Jr, R., Roberts,  
259 C.J., Elsheikh, A., 2019. Determination of corneal biomechanical behavior in-vivo for healthy eyes  
260 using CorVis ST tonometry: stress-strain index. *Front. Bioeng. Biotechnol.* 7, 105.
- 261 Elsheikh, A., Brown, M., Alhasso, D., Rama, P., Campanelli, M., Garway-Heath, D., 2008. Experimental  
262 assessment of corneal anisotropy. *J. Refract. Surg. Off. Publ. Int. Soc. Refract. Surg.* 24.
- 263 Elsheikh, A., Alhasso, D., Rama, P., 2008. Biomechanical properties of human and porcine corneas.  
264 *Exp. Eye Res.* 86, 783–790. <https://doi.org/10.1016/j.exer.2008.02.006>
- 265 Elsheikh, A., Geraghty, B., Rama, P., Campanelli, M., Meek, K.M., 2010. Characterization of age-related  
266 variation in corneal biomechanical properties. *J. R. Soc. Interface* 7, 1475–1485.
- 267 Elsheikh, A., Kassem, W., Jones, S.W., 2011. Strain-rate sensitivity of porcine and ovine corneas. *Acta*  
268 *Bioeng. Biomech.* 13.

- 269 Hamon, L., Daas, L., Mäurer, S., Weinstein, I., Quintin, A., Schulz, K., Langenbucher, A., Seitz, B., 2021.  
270 Thickness and Curvature Changes of Human Corneal Grafts in Dextran-Containing Organ Culture  
271 Medium Before Keratoplasty. *Cornea* 40, 733–740.  
272 <https://doi.org/10.1097/ICO.0000000000002543>
- 273 Hoeltzel, D.A., Altman, P., Buzard, K., Choe, K. II, 1992. Strip extensimetry for comparison of the  
274 mechanical response of bovine, rabbit, and human corneas. *J. Biomech. Eng.* 114, 202–215.  
275 <https://doi.org/10.1115/1.2891373>
- 276 Kling, S., Khodadadi, H., Goksel, O., 2020. Optical Coherence Elastography-Based Corneal Strain  
277 Imaging During Low-Amplitude Intraocular Pressure Modulation. *Front. Bioeng. Biotechnol.* 7.  
278 <https://doi.org/10.3389/fbioe.2019.00453>
- 279 Labate, C., Lombardo, M., De Santo, M.P., Dias, J., Ziebarth, N.M., Lombardo, G., 2015. Multiscale  
280 investigation of the depth-dependent mechanical anisotropy of the human corneal stroma.  
281 *Investig. Ophthalmol. Vis. Sci.* 56, 4053–4060. <https://doi.org/10.1167/iovs.15-16875>
- 282 Mahdian, M., Seifzadeh, A., Mokhtarian, A., Doroodgar, F., 2021. Characterization of the transient  
283 mechanical properties of human cornea tissue using the tensile test simulation. *Mater. Today*  
284 *Commun.* 26, 102122. <https://doi.org/10.1016/j.mtcomm.2021.102122>
- 285 Meek, K.M., Leonard, D.W., Connon, C.J., Dennis, S., Khan, S., 2003. Transparency, swelling and  
286 scarring in the corneal stroma. *Eye* 17, 927–936. <https://doi.org/10.1038/sj.eye.6700574>
- 287 Nambiar, M.H., Liechti, L., Müller, F., Bernau, W., Studer, H., Roy, A.S., Seiler, T.G., Büchler, P., 2022.  
288 Orientation and depth dependent mechanical properties of the porcine cornea: Experiments and  
289 parameter identification. *Exp. Eye Res.* 224, 109266.  
290 <https://doi.org/10.1016/j.exer.2022.109266>
- 291 Pandolfi, A., Manganiello, F., 2006. A model for the human cornea: Constitutive formulation and  
292 numerical analysis. *Biomech. Model. Mechanobiol.* 5, 237–246. <https://doi.org/10.1007/s10237->



293 005-0014-x

294 Petsche, S.J., Chernyak, D., Martiz, J., Levenston, M.E., Pinsky, P.M., 2012. Depth-dependent  
295 transverse shear properties of the human corneal stroma. *Investig. Ophthalmol. Vis. Sci.* 53, 873–  
296 880. <https://doi.org/10.1167/iovs.11-8611>

297 Quantock, A.J., Boote, C., Young, R.D., Hayes, S., 2007. Small-angle fibre diffraction studies of corneal  
298 matrix structure: a depth-profiled investigation of the human eye-bank cornea 335–340.  
299 <https://doi.org/10.1107/S0021889807005523>

300 Ramirez-Garcia, M.A., Sloan, S.R., Nidenberg, B., Khalifa, Y.M., Buckley, M.R., 2018. Depth-Dependent  
301 Out-of-Plane Young's Modulus of the Human Cornea. *Curr. Eye Res.* 43, 595–604.  
302 <https://doi.org/10.1080/02713683.2017.1411951>

303 Randleman, J.B., Dawson, D.G., Grossniklaus, H.E., McCarey, B.E., Edelhauser, H.F., 2008. Depth-  
304 dependent cohesive tensile strength in human donor corneas: Implications for refractive  
305 surgery. *J. Refract. Surg.* 24, 20080101. <https://doi.org/10.3928/1081597x-20080101-15>

306 Roberts, C.J., 2016. Importance of accurately assessing biomechanics of the cornea. *Curr. Opin.*  
307 *Ophthalmol.* 27, 285–291. <https://doi.org/10.1097/ICU.0000000000000282>

308 Sinha Roy, A., Dupps, W.J., Roberts, C.J., 2014. Comparison of biomechanical effects of small-incision  
309 lenticule extraction and laser in situ keratomileusis: Finite-element analysis. *J. Cataract Refract.*  
310 *Surg.* 40, 971–980. <https://doi.org/10.1016/j.jcrs.2013.08.065>

311 Sloan, S.R., Khalifa, Y.M., Buckley, M.R., 2014. The location- and depth-dependent mechanical  
312 response of the human cornea under shear loading. *Investig. Ophthalmol. Vis. Sci.* 55, 7919–  
313 7924. <https://doi.org/10.1167/iovs.14-14997>

314 Studer, H., Larrea, X., Riedwyl, H., Büchler, P., 2010. Biomechanical model of human cornea based on  
315 stromal microstructure. *J. Biomech.* <https://doi.org/10.1016/j.jbiomech.2009.11.021>

- 316 Sun, B., 2021. The mechanics of fibrillar collagen extracellular matrix. *Cell Reports Phys. Sci.* 2.  
317 <https://doi.org/10.1016/j.xcrp.2021.100515>
- 318 Wang, J., Simpson, T.L., Fonn, D., 2004. Objective measurements of corneal light-backscatter during  
319 corneal swelling, by optical coherence tomography. *Investig. Ophthalmol. Vis. Sci.* 45, 3493–  
320 3498. <https://doi.org/10.1167/iovs.04-0096>
- 321 Wolf, A.H., Welge-Lüen, U.C., Priglinger, S., Kook, D., Grueterich, M., Hartmann, K., Kampik, A.,  
322 Neubauer, A.S., 2009. Optimizing the deswelling process of organ-cultured corneas. *Cornea* 28,  
323 524–529. <https://doi.org/10.1097/ICO.0B013E3181901DDE>
- 324 Wollensak, G., Spoerl, E., Seiler, T., 2003. Stress-strain measurements of human and porcine corneas  
325 after riboflavin-ultraviolet-A-induced cross-linking. *J. Cataract Refract. Surg.* 29, 1780–1785.  
326 [https://doi.org/10.1016/S0886-3350\(03\)00407-3](https://doi.org/10.1016/S0886-3350(03)00407-3)
- 327
- 328

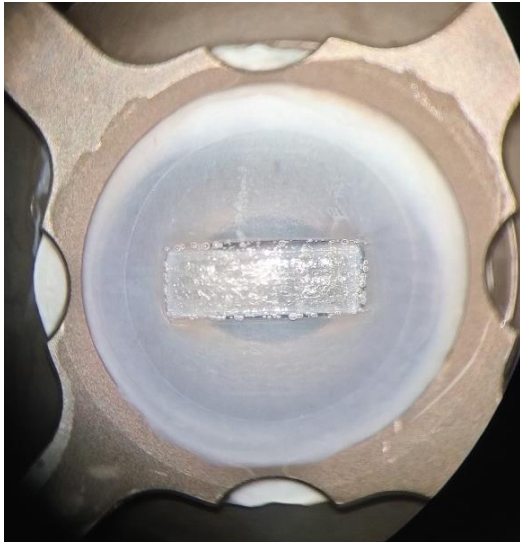
Depth	A (MPa)	B (-)	$\varepsilon_0$
D1	64.20 $10^{-3}$	25.28	11.19 $10^{-3}$
D2	47.41 $10^{-3}$	25.54	14.35 $10^{-3}$
D3	25.64 $10^{-3}$	26.74	22.37 $10^{-3}$

329 **Table 1:** The estimated parameters from the exponential fitting of the experimental stress strain data  
330 showed a linear decrease in parameter 'A' while parameter 'B' remained relatively constant.  
331 Parameter  $\varepsilon_0$  was obtained to account for the prestress in the experimental condition at 0 strain.

332

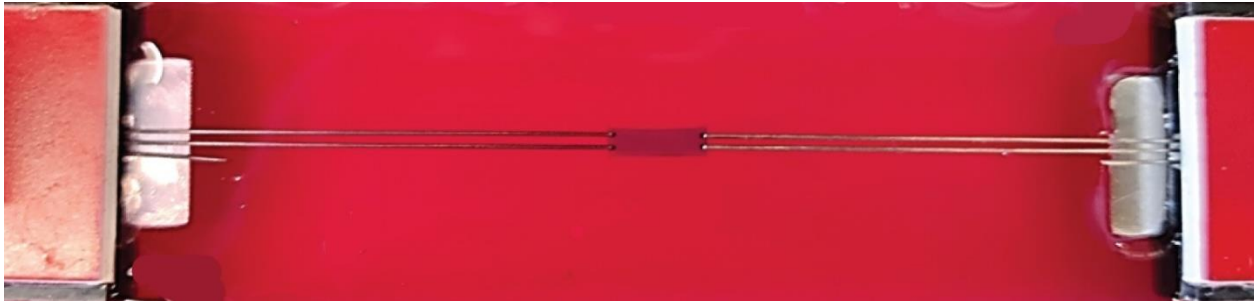
Journal Pre-proof

333



334

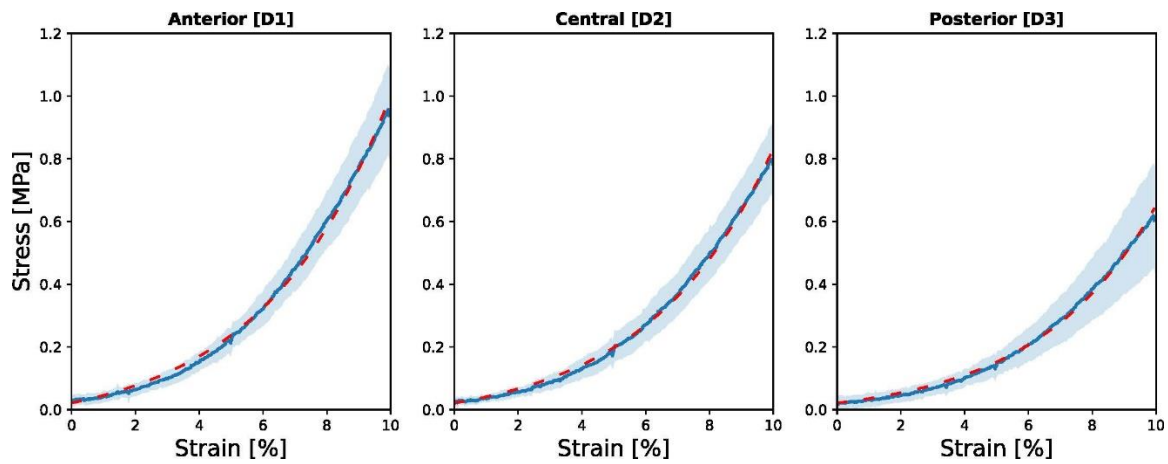
335 **Figure 1:** The cornea with scleral rim, clamped in an artificial chamber showing the strips cut out in  
336 the mid corneal region.



337

338 **Figure 2:** The corneal strip (6 x 2 x 0.15 mm) was tested under traction in a bath of MEM + 5%  
339 dextran with BioRake attachments. Note that one of the tins has been cut on both sides to leave  
340 only two for sample attachment.

Journal Pre-proof



341

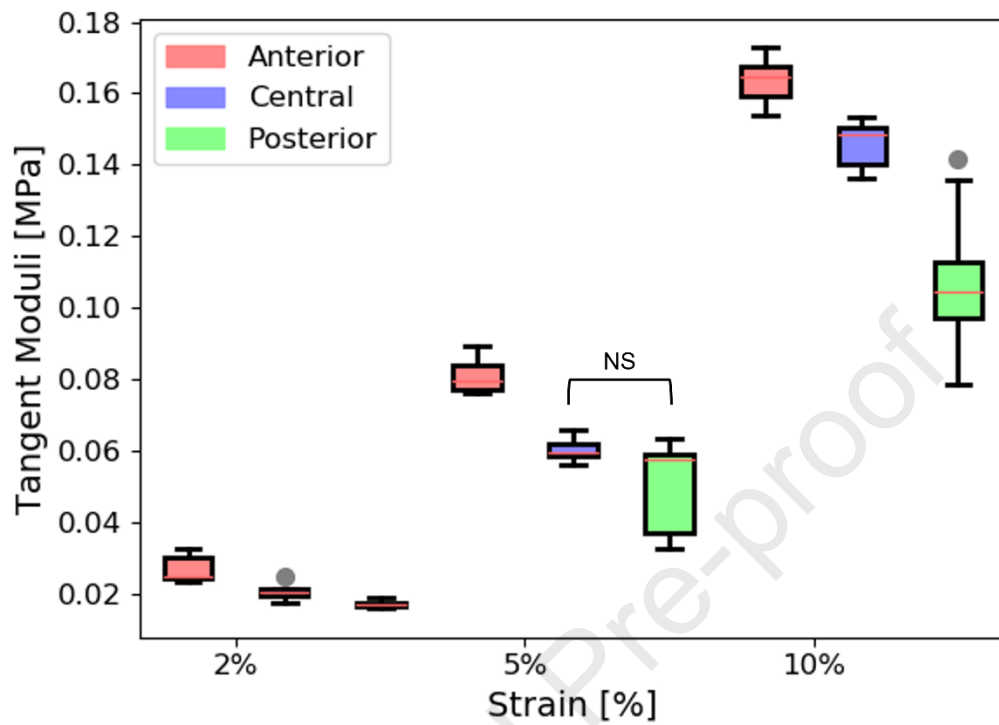
342 **Figure 3:** The Stress-Strain reaction of the strips in the anterior (D1, n=7), central (D2, n=8) and  
343 posterior (D3, n=8) groups. The solid blue line represents the mean stress, and the shaded region  
344 represents the standard deviation. The dashed red line represents the exponential fit with equation  
345 1.

346

347

348

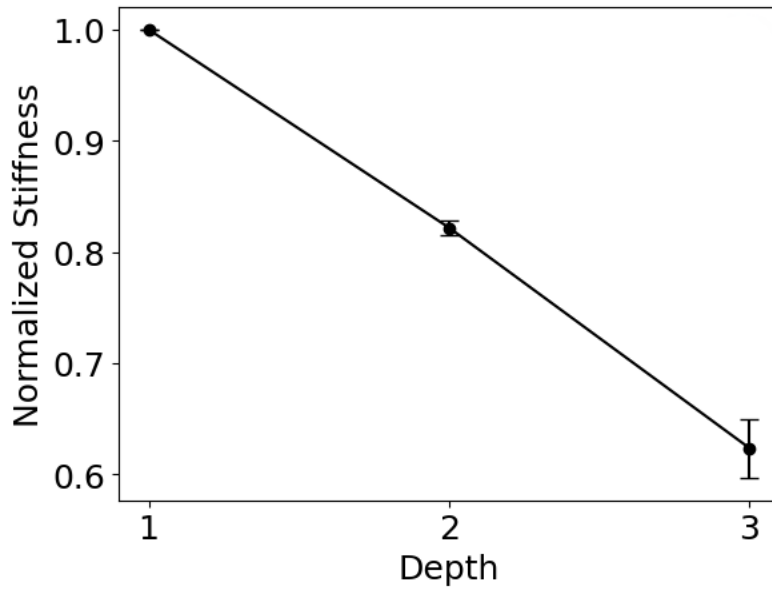
349



350

351 **Figure 4:** The tangent moduli in the anterior (D1, n=7), central (D2, n=8) and posterior (D3, n=8)  
352 groups, for 2%, 5% and 10 % strain. All groups except indicated (NS,  $p = 0.051$ ) show a significant  
353 difference ( $p < 0.05$ ).

354



355  
356

357 **Figure 5:** The stiffness calculated based on the exponential fit at each depth was normalized with  
358 respect to the stiffness of the anterior layer. This normalized stiffness ratio showed a linearly  
359 decreasing stiffness from the anterior to the posterior part of the cornea.



## Highlights

- Human cornea shows depth-dependent mechanical properties, with a linear decrease in tensile mechanical properties from the anterior to the posterior cornea.
- The tangent moduli at different strains show significant differences across the depth of the cornea.
- While full-thickness studies have been previously performed, this to the best of our knowledge, is the first depth-dependent analysis in uniaxial extension of the human cornea

Journal Pre-proof